

# The Local Hole in the Galaxy Distribution: Evidence from 2MASS

W.J. Frith, G.S. Buswell, R. Fong, N. Metcalfe & T. Shanks

*Department of Physics, University of Durham, Science Laboratories, South Road, Durham, DH1 3LE, United Kingdom*

3 July 2018

## ABSTRACT

Using the bright galaxy counts from the 2 Micron All Sky Survey (2MASS) second incremental release, two techniques for probing large-scale structure at distances of  $\sim 150 h^{-1}$  Mpc are investigated. First, we study the counts from two sets of six  $5^\circ \times \sim 80^\circ$  strips in the two galactic caps. In the six southern strips a deficit of  $\sim 30$  per cent was found relative to a predicted homogeneous distribution at  $K_s \sim 11$ . These strips were also in good agreement with a model incorporating the radial density function of the southern 2dF Galaxy Redshift Survey (2dFGRS), which shows a deep underdensity between  $\sim 90$  and  $180 h^{-1}$  Mpc. Together with a similar underdensity found in the Las Campanas Redshift Survey, these results indicate a very large ‘local hole’ in the Southern Galactic Cap (SGC) to  $\gtrsim 150 h^{-1}$  Mpc with a linear size across the sky of  $\sim 200 h^{-1}$  Mpc but with a significantly lower mean underdensity of  $\sim 30$  per cent than that suggested by the bright APM SGC counts. The counts in the northern set of strips are low overall but indicate a more varied pattern. When all the available 2MASS data with  $|b| > 30^\circ$  were aggregated, they indicated underdensities of  $\sim 18$  per cent and  $\sim 30$  per cent at  $K_s \sim 11$  for the northern and southern areas respectively. Our second method uses the ratio of the counts with  $11.38 < K_s < 12.38$  to  $12.88 < K_s < 13.38$  binned in  $25 \text{ deg}^2$  areas; the counts from these areas provide a smoothed map over the sky of the slope in the counts between  $K_s=11.38$  and  $13.38$ . Visually, the resulting map shows the expected complex form of the cosmic web and picks out known rich clusters, demonstrating the usefulness of this ‘slope statistic’ as a probe of large-scale structure at distances of  $\lesssim 150 h^{-1}$  Mpc. Most interestingly, the map also shows large regions,  $\sim 100^\circ$  across, of steep counts in both hemispheres. Thus, the present 2MASS data suggest the presence of a potentially huge contiguous void stretching from south to north. Not only would this delineate further the limits for the Cosmological Principle but it would also show the possible presence of significant power on scales of  $\gtrsim 300 h^{-1}$  Mpc in the galaxy power spectrum.

**Key words:** surveys - galaxies: photometry - cosmology: observations - large-scale structure of Universe - infrared: galaxies

## 1 INTRODUCTION

Over the last twenty years, our understanding of the galaxy distribution in the local universe has advanced dramatically. The observational success since the 1920s of Friedmann universes reflects a fundamental aspect of the Universe, its isotropy and homogeneity, expressed theoretically by the Cosmological Principle. Indeed, it is in the context of Friedmann universes that recent observations of the cosmic microwave background, SNIa and galaxy redshift surveys provide evidence for a non-zero cosmological constant. On the other hand, the observations of large-scale structure in the galaxy distribution shows that on even quite large scales

the Universe is highly inhomogeneous, with the galaxy distribution tracing out a cosmic web of filamentary and wall-like structures.

Thus, the question arises as to the scales on which the Universe can be viewed as isotropic and homogeneous, i.e., the scales at which the Cosmological Principle can be said to hold. Recent work on the local distribution of galaxies indicates the existence of ‘great walls’ of  $\sim 100 h^{-1}$  Mpc in size and  $\sim 30\text{--}50 h^{-1}$  Mpc voids (e.g. Bellanger & De Lapparent, 1995). These observations would seem to support the possibility that the steeper than expected APM  $B$ -band galaxy counts over  $4300 \text{ deg}^2$  of the Southern Galactic Cap (SGC) might indeed reflect a very large local hole in the Universe

(Shanks 1990). But for our present understanding of the cosmic web, as gathered from dynamical N-body simulations, it would be unexpectedly large and deep (Baugh et al., 2002). Such a local hole would clearly place stringent constraints on any model of large-scale structure. However, using CCD photometry Metcalfe, Fong & Shanks (1995) found a small residual scale error in the APM zero-points for  $B \gtrsim 17$ . The corrected APM counts fainter than  $B \sim 17.5$  were now in good agreement with the expected counts from normal homogeneous models; a deficit of  $\sim 50$  per cent at  $B \sim 15.5$  still remained along with the possibility of a very large deep hole in the SGC.

The presence of an underdensity in the SGC is now being corroborated by preliminary results from deep galaxy redshift surveys, probing the galaxy distribution to  $z \sim 0.2$ . The number-redshift histograms,  $n(z)$ , of the Southern surveys display astonishing structures, with large regions of underdensity at  $z \sim 0.03$ – $0.06$  bounded by sharp peaks of overdensity (Zucca et al., 1997; Shectman et al. 1996; Ratcliffe et al., 1996; Norberg et al., 2002).

Interestingly, the 2 Micron All Sky Survey (2MASS; Jarrett et al., 2000) is in the process of completing an infrared survey of the whole sky. Even with the preliminary data released by 2MASS it is possible to test the observational results indicating a large hole. In particular, compared with the photographic APM survey, a survey based on digital photometry has fewer concerns over errors in the calibration and field-to-field variations in the zero-point and limiting magnitude. However, a complete interpretation of the 2MASS infrared counts is at present hindered by uncertainties in the surveyed area arising from the incompleteness of the survey and an intricate mask not yet publicly available.

With the goal of determining the approximate variations in the galaxy distribution over the galactic caps, and the scale of local large-scale inhomogeneities, we have thus compared the  $K_s$ -band 2MASS counts from several declination strips over the galactic caps with models incorporating the radial density functions of the 2dF Galaxy Redshift Survey (2dFGRS; Colless et al., 2001), in their northern and southern areas. To see if the features seen in these strips persisted over larger solid angles we then examined the combined available counts for  $|b| \geq 30^\circ$ . For a more detailed view of these inhomogeneities, we used variations in the slope of the 2MASS counts between  $K_s = 11.38$  and  $13.38$  as a probe of inhomogeneities on scales of  $\sim 5^\circ$ . In Section 2 we present general details of the data samples used. In Section 3 we first examine the optical magnitude counts from the APM survey and 2dFGRS, and then carry out the aforementioned analyses of the 2MASS data. The results are summarised and discussed in Section 4.

## 2 THE DATA

### 2.1 The APM Survey

The APM survey is the largest complete galaxy survey to date, covering a contiguous  $\sim 4300$  deg<sup>2</sup> area in the SGC, with 20 million images brighter than  $b_j = 22$ . It is based on the APM photometry of 185 photographic Schmidt plates in the region  $\alpha \sim 21^h$  to  $5^h$  and  $\delta \sim -70^\circ$  to  $-20^\circ$  (Maddox et al., 1990a,b). As mentioned in section 1, the Metcalfe et

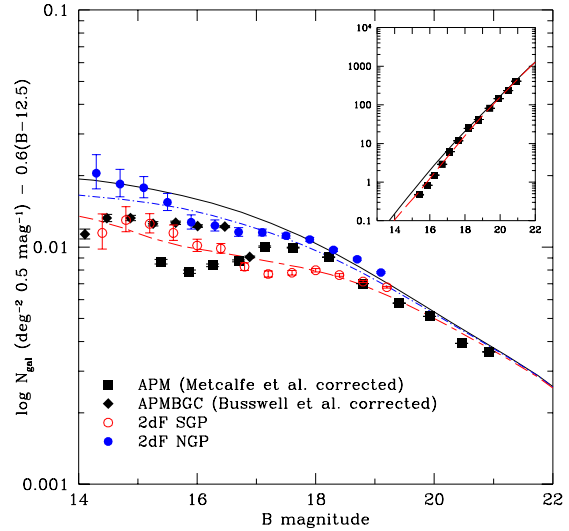


**Figure 1.** Magnitude counts from the Metcalfe et al. corrected APM survey (Maddox et al., 1990a,b), the Busswell et al. corrected APMBGC and 2dF parent catalogue counts for the northern and southern fields (Norberg - priv. comm.); the errorbars indicated are Poissonian. The main diagram indicates the counts with a subtracted Euclidean slope; the inset shows the Metcalfe et al. corrected APM counts on an ordinary logarithmic scale for reference. The continuous line represents the expected homogeneous trend, while the dashed and dot-dashed lines show the models derived from the 2dF radial density profiles for  $B \leq 17.5$  in the southern and northern fields respectively as calculated from Figs. 2 and 3.

al. (1995) corrections to the APM photometry are used here with a mean colour correction of  $B - b_j = 0.2$ .

We have also used the publicly available APM Bright Galaxy Catalogue (APMBGC; Loveday et al., 1996), which reaches a magnitude limit of  $b_j = 16.44$ . Using very accurate photometric data taken from the CTIO over the approximate current 2dFGRS declination strips, a zero-point correction of 0.313 magnitudes, found from over 700 matched galaxies, has been applied to these counts (Busswell et al., 2002).

### 2.2 The 2dF Galaxy Redshift Survey

The 2dFGRS is selected in the photographic  $b_j$  band using the APM survey and subsequent alterations and extensions to it (Norberg et al., 2002) for two declination strips in the northern and southern galactic caps, as well as 99 randomly selected  $2^\circ$  fields scattered over the southern APM field. The data used in this paper is taken from the 100k data release detailed in Colless et al. (2001), which has made spectroscopic and photometric data publicly available for  $\sim 90,000$  galaxies in the SGC and NGC, bounded approximately by  $\alpha \sim 22^h$  to  $3^h 30^m$  and  $\delta \sim -32^\circ$  to  $-26^\circ$  in the southern declination strip and  $\alpha \sim 10^h 20^m$  to  $13^h 40^m$  and  $\delta \sim -6^\circ$  to  $0^\circ$  in the NGC. Despite the fact that the original 2dFGRS galaxy sample was selected with an extinction-corrected limit of  $b_j = 19.45$ , subsequent linearity and zero-

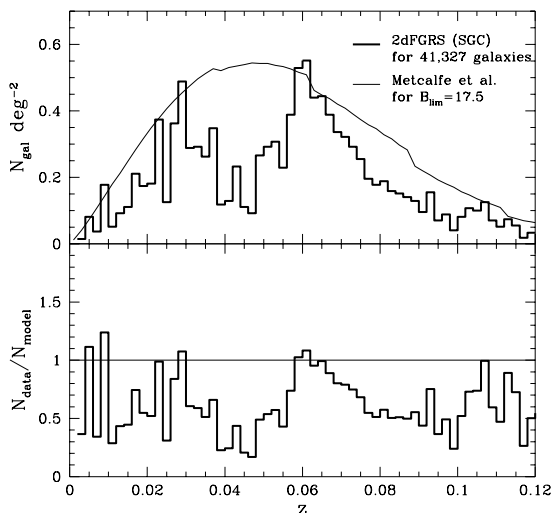


**Figure 2.** The galaxy redshift distribution for 41,327 galaxies from the 2dFGRS SGC declination strip. The top figure shows the number of galaxies per redshift bin per square degree; the data is normalised such that the ratio of the number of galaxies predicted by the model to the observed number matches the corresponding ratio in the 2dF SGP counts shown in fig. 1. The continuous line indicates the expected trend calculated from the PLE model detailed in section 3.1 for  $B_{lim} = 17.5$ , using a blanket colour correction of  $B - b_j = 0.2$  to transfer the 2dF parent catalogue to the  $B$ -band. The bottom figure shows the radial density profile for this data.

point recalibrations of the 2dF parent catalogue, as well as revised extinction estimates over the 2dF fields, result in median limiting magnitudes of  $b_j = 19.40$  over the SGC field, and  $b_j = 19.35$  in the NGC field. The 2dF galaxy data used in this paper has been selected with a quality flag of  $Q \geq 3$  corresponding to a redshift reliability of  $>90$  per cent for 92.7 per cent of the total sampled galaxies (Colless et al. 2001).

### 2.3 The 2MASS Extended Source Catalogue

The 2 Micron All Sky Survey (2MASS) is a digital survey of the whole sky in the  $K_s$ ,  $J$  and  $H$ -bands. Through the 2MASS second incremental release the photometry for  $\sim 6 \times 10^5$  galaxies is publicly available with a complete detection rate to  $K_s = 13.5$  (Jarrett et al., 2000).

The  $K_s$ -band magnitudes used in this paper have been determined using the method of Cole et al. (2001). In a comparison with the deeper  $K$  photometry of Loveday (2000), Cole et al. found that the most accurate  $K_s$  Kron magnitudes are obtained from the 2MASS  $J$ -band Kron magnitudes, colour corrected using the  $J - K$  default aperture colours, with a zero-point offset of 0.061 mag. An additional correction is also needed to convert these Kron magnitudes to total magnitudes; a blanket 0.12 mag correction was applied to account for this and the zero-point offset. A full account of these corrections can be found in Cole et al.

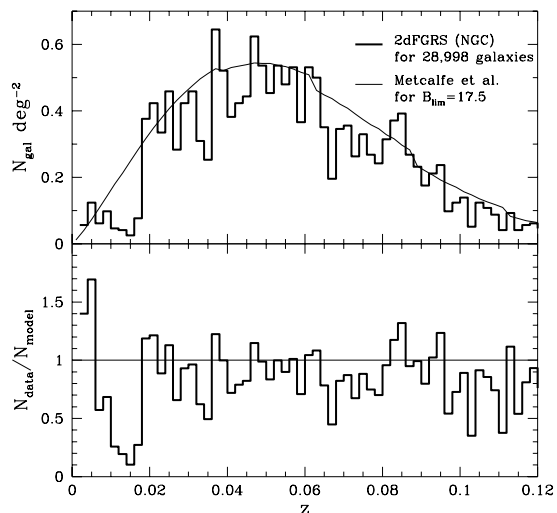


**Figure 3.** The galaxy redshift distribution for 28,998 galaxies in the 2dFGRS NGC equatorial field. Again the top figure shows the number of galaxies per redshift bin per square degree; the data has been normalised in the same way as the southern distribution. The continuous line indicates the expected trend for  $B_{lim} = 17.5$ , again using the blanket  $B - b_j = 0.2$  colour correction but with an additional zero-point correction of 0.1 mag. found by Busswell et al. (2002) for the northern field with respect to their CTIO northern photometry; the residual  $B - b_j$  correction to the 2dF parent catalogue is 0.1 mag. The bottom figure shows the radial density profile for this data.

## 3 BRIGHT GALAXY COUNTS

### 3.1 Optical galaxy counts

The originally published APM galaxy counts for the SGC show a steeper than expected slope brightward of  $B \sim 19$  (Maddox et al., 1990). Subsequent studies by Metcalfe et al. (1995) have revealed a scale error in the original APM photometry for  $17 < B < 19$ , yielding counts faintward of  $B = 18$  which are more consistent with a homogeneous model for the universe. However, the galaxy counts are still very low brightward of  $B \sim 18$  (with a galaxy count of  $\sim 50$  per cent with respect to the homogeneous prediction at  $B \sim 15.5$  mag.), and the photometry here is uncertain. However new photometry checks of the APMBGC (Loveday et al., 1996) with very accurate CTIO photometry over the approximate 2dF declination fields (Busswell et al., 2002) indicate a 0.313 mag. zero-point correction to the bright photometry yielding APM counts for  $B < 17$  which are higher but still significantly underdense (a galaxy count of  $\sim 75$  per cent with respect to the homogeneous prediction at  $B \sim 15.6$  mag.). Fig. 1 shows the APM SGC counts with the Metcalfe et al. corrections, and the Busswell et al. corrected APMBGC counts using a colour correction to the  $B$ -band of  $B - b_j = 0.2$ . Similar comparisons of the Busswell et al. CTIO photometry with the 2dF parent catalogue indicate a mean 0.1 magnitude zero-point error over the northern field such that the 2dF magnitudes are too faint, and a negligible off-set in the south; the corrected 2dF parent catalogue

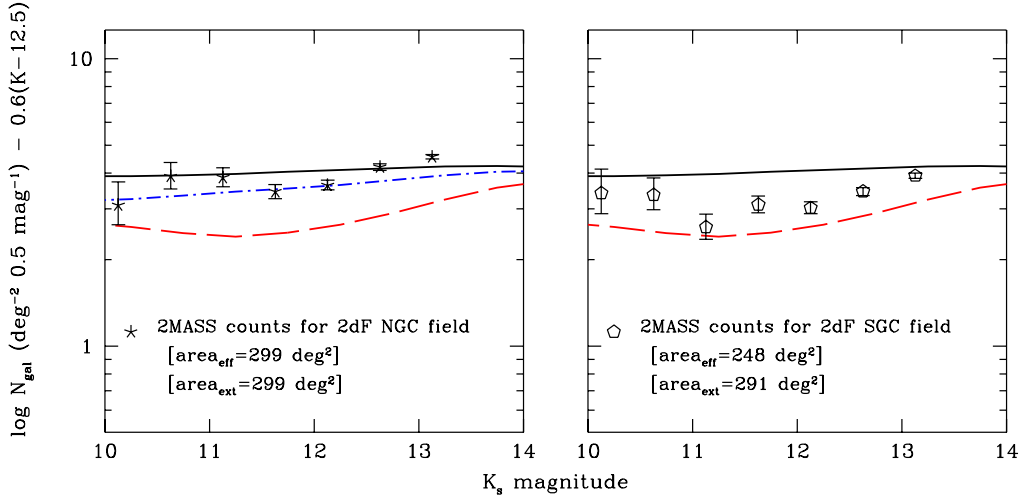


**Figure 4.** Galaxy magnitude counts extracted from 2MASS for the approximate current 2dF declination fields. The appropriate  $K$ -band models are indicated, with the homogeneous counts indicated by the solid line, the 2dF SGC model with the dashed line and the 2dF NGC model by a dot-dashed line as in fig. 1. The effective and extracted areas are also shown, corresponding to the solid angle of the selected field and the calculated solid angle accounting for gaps in the data.

counts (Norberg - priv. comm.) are also shown using the same  $B - b_j$  colour correction. The models shown in Fig. 1 are based on the Pure Luminosity Evolution (PLE) model of Metcalfe et al. (2001) incorporating a  $K + E$ -correction detailed in Bruzual & Charlot (1993).

Recent redshift surveys are beginning to elucidate the cause of the steeper than expected slope of bright galaxy counts. Fig. 2 and Fig. 3 show the 2dFGRS redshift distributions in the upper panels and the radial density profiles below for the 100k data release (Colless et al., 2001) for the southern and northern declination fields respectively. We have imposed a limiting magnitude of  $B_{lim}=17.5$  in order to more accurately match the 2MASS limiting  $K$ -band magnitude and therefore probe a similar redshift range. The 2dF data are compared to an expected homogeneous distribution using the Metcalfe et al. (2001) PLE prediction. In order to avoid uncertainties in the effective area and redshift completeness the data has been normalised such that the ratio of predicted to observed galaxies is equal to the ratio of the corresponding cumulative 2dF counts to the cumulative number of galaxies predicted by the homogeneous number count model for  $B \leq 17.5$ . Most striking in the southern distribution is the visible large-scale structure, characterised by deficiencies at  $0.03 \lesssim z \lesssim 0.06$  ( $\sim 90$  to  $180 h^{-1}$  Mpc) and  $z \lesssim 0.06 z \lesssim 0.1$  ( $\sim 180$  to  $300 h^{-1}$  Mpc). The NGC field also indicates a deficiency below  $z \sim 0.02$ , beyond which the distribution is approximately homogeneous.

We first wish to check if the observed 2dF galaxy distributions in the SGC and NGC might explain the low southern galaxy-magnitude counts, and the apparent asymmetry between the north and south. Incorporating the radial density profiles from the 2dF areas (the ratio of the observed distribution to the expected homogeneous counts from Figs. 2 and 3) into the homogeneous model as a coefficient of the

luminosity function parameter  $\phi^*$ , yields an expected trend for the corresponding galaxy-magnitude counts. For  $z > 0.12$  a constant, homogeneous  $\phi^*$  is used). The dot-dashed and dashed lines in Fig. 1 show the predictions of these variable  $\phi^*$  models for the northern and southern 2dF counts respectively. The observed 2dF counts and the corresponding models show excellent agreement.

The low trends of the 2dF SGC counts and the APM  $B > 17$  and APMBGC  $B < 17$  counts imply significant structure especially since the APM southern field covers  $\sim 4300 \text{ deg}^2$ . The presence of significant large-scale structure is also indicated in the Southern  $n(z)$  of the Las Campanas Redshift Survey (Shectman et al. 1996), which samples an area of  $7.5^\circ \times 80^\circ$  in the SGC  $\sim 15^\circ$  southward of the 2dF area. The 2dF NGC variable  $\phi^*$  model and 2dF NGC counts are low but indicate a much smaller deficiency in the counts. This can be observed in the 2dF NGC  $n(z)$  (Fig. 3) which is closer to the homogeneous prediction.

This apparent asymmetry in the SGC and NGC  $n(z)$  and the scale and distance of the SGC inhomogeneities are intriguing, and can be further investigated using the presently released 2MASS data.

### 3.2 2MASS galaxy counts

The asymmetry observed in the SGC and NGC optical magnitude counts and 2dFGRS  $n(z)$  can be further investigated using the 2MASS second incremental release. Firstly, we wish to examine the trend of the  $K$ -band counts for the 2dF fields to determine whether the observed deficiencies and north-south asymmetry is present in the  $K$ -band, and also to verify the usefulness of the variable  $\phi^*$  models described in Section 3.1. Fig. 4 shows the 2MASS  $K_s$  counts extracted from the approximate 2dF 100k data release fields

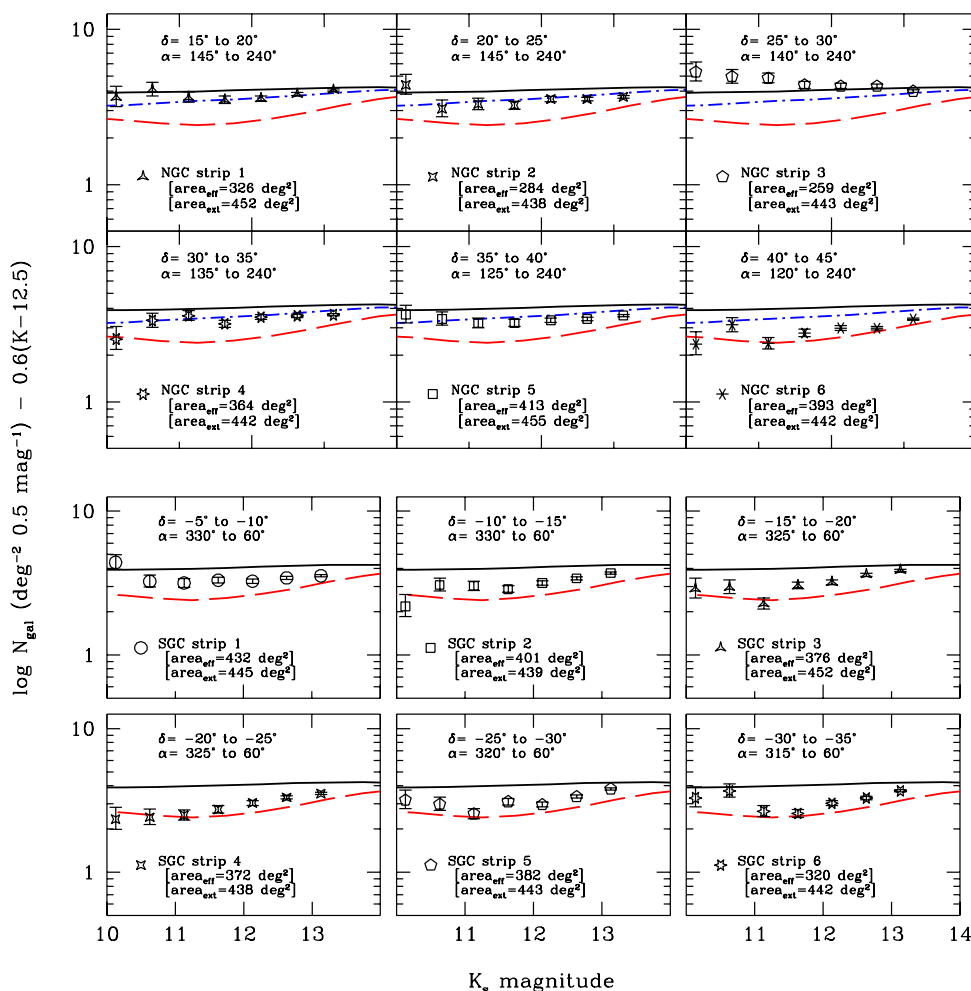


**Figure 5.** Magnitude counts extracted from 2MASS in declination strips each 5 degrees wide from the NGC and SGC, shown in the top and bottom panels respectively. Again the counts are shown with the Euclidean slope subtracted and with Poisson errors. The homogeneous PLE model is indicated by the continuous line, the model derived from the southern 2dF radial density profile for  $B \leq 17.5$  is shown in all strips by a dashed line, and the northern model is indicated in the northern strips by a dot-dashed line. The effective and extracted areas are also indicated for each strip.

for which 2MASS data is available. Also shown are the homogeneous prediction and the variable  $\phi^*$  models for the 2dFGRS SGC and NGC fields using the radial density function for  $B \leq 17.5$  (approximately matching the limiting  $K_s$  magnitude of 2MASS and therefore more likely to produce a better description of the counts).

Unfortunately, the 2MASS mask for the second incremental release is fairly complex and the effective areas had to be determined approximately. This was carried out by searching for gaps in the 2MASS astrometry of over 0.5 degrees on the right ascension axis in 0.5 degree declination strips; the maximum right ascension range of any missing area was then determined. The declination range of unobserved areas was similarly inferred yielding an upper limit on the area of the missing region. A visual inspection of the distribution of the 2MASS galaxies on the sky reveals that

this estimate of the effective area is likely to be reasonably good for fairly complete strips.

The resulting  $K_s$  counts are in excellent agreement with the  $B$ -band 2dF counts; comparing the counts at approximately equivalent magnitudes, the northern counts indicate deficiencies of 0.0 per cent (at  $B = 15.1$ ) and 2.7 per cent (at  $K_s = 11.13$ ), and the southern counts deficiencies of 28 per cent (at  $B = 15.2$ ) and 32 per cent (at  $K_s = 11.13$ ). The  $K_s$  counts for the 2dF fields are also in approximate agreement with the predictions of the corresponding variable  $\phi^*$  models.

Together with the structure seen in the 2dF  $n(z)$ , these 2MASS  $K_s$  counts show that such bright counts in areas as small as  $\sim 300 \text{ deg}^2$  can be used as a diagnostic probe of large underdensities at distances of  $\sim 150 h^{-1} \text{ Mpc}$  since the slope of the counts between  $K_s \sim 11$  and  $K_s \sim 13$  is dependent on the redshift distribution at these distances; small

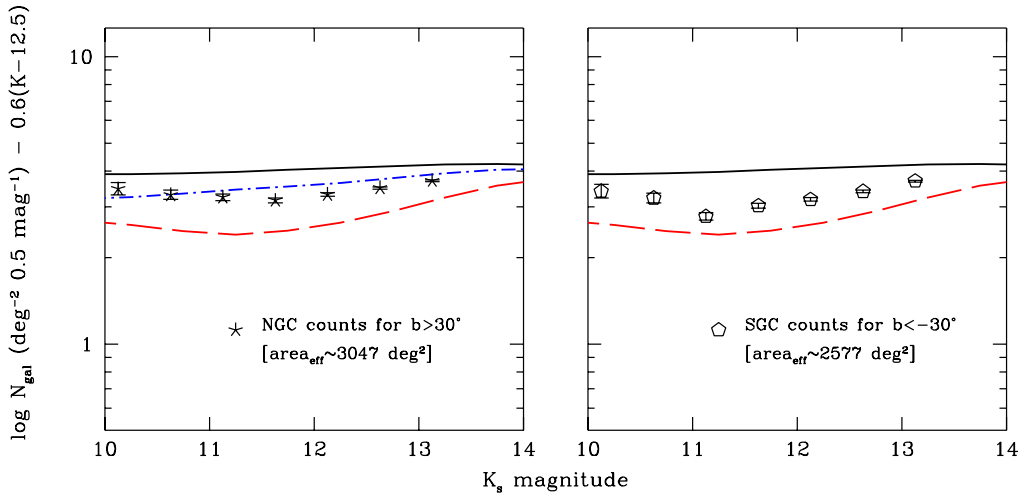


**Figure 6.** Galaxy magnitude counts extracted from 2MASS for the northern ( $b \geq 30^\circ$ ) and southern ( $b \leq -30^\circ$ ) galactic caps. The counts here are normalised to the mean number seen in the corresponding set of strips at  $K_s = 13.13$ . The appropriate models are indicated as in fig. 4. The effective areas indicated here correspond to the effective solid angle inferred by the normalisation.

fluctuations in the galaxy distribution at greater distances have little effect on the number counts at these magnitudes (Frith 2001).

Using this comparison between bright counts and the 2dF variable  $\phi^*$  models, it is now possible to investigate the angular extent of the local hole in the SGC using 2MASS. To this end, the counts were determined for six 5 degree declination strips in the SGC (Fig. 5), each with approximately the same solid angle and right ascension range as the current 2dF fields (see Fig. 4). In order to determine the robustness of the north–south asymmetry observed in the 2dF survey and the corresponding  $B$  and  $K_s$  band counts, 2MASS counts were also taken for another six similar strips in the NGC. The number and positions of these strips were restricted firstly by the constraints of the mask of the available 2MASS data, and secondly by regions of significant extinction; declinations with  $|b| \geq 30^\circ$  were selected.

The southern strip counts in Fig. 5 are in approximate agreement with the 2dF SGC variable  $\phi^*$  model with a uniform steep slope in the counts over the entire declination range, similar to the 2MASS counts for the 2dF SGC field (Fig. 4), indicating that the ‘local hole’ extends as far north as  $\delta = 0^\circ$  in the SGP, and as far south as can be sampled with the present 2MASS catalogue. Considering that the LCRS  $n(z)$  (Shectman et al. 1996) indicates a similar underdensity at  $\sim 150 h^{-1}$  Mpc,  $\sim 15^\circ$  south of the 2dF SGP field, it would seem to support the presence of a ‘local hole’ in the SGC of at least  $\sim 80^\circ \times 40^\circ$  in extent ( $\sim 65$  per cent of the APM SGC area).

In the northern strips, the counts in Fig. 5 are more varied with approximate agreement with the 2dF NGC variable  $\phi^*$  model and the form of the 2MASS counts for the 2dF NGC field in all but two strips. The shallow counts in the third strip ( $25^\circ < \delta < 30^\circ$ ) are probably due to the presence of the Coma cluster and its associated supercluster.

In the strip counts of both hemispheres, similar mean deficiencies for the southern and northern aggregated counts at  $K_s = 13.13$  of  $\sim 12$  per cent are found corresponding to a mean depth of  $\geq 150 h^{-1}$  Mpc, possibly indicating that the inhomogeneities in the local galaxy distribution exist on larger scales.

It is worth noting that the slopes of the counts in the northern strips in Fig. 5 are fairly close to Euclidean, and that a renormalisation of the model or a 10 per cent error in the effective areas would compensate for the apparent deficiency. However, these compensation effects are likely to be fairly small since, firstly, any change in the model normalisation would affect the excellent agreement the model has with fainter K-band data (e.g. Gardner et al., 1996; Huang et al., 1996; Glazebrook et al., 1995), and secondly, since any significant recalculation of the effective areas would upset the excellent agreement of the 2dF optical magnitude counts with the 2MASS counts for the 2dF fields (Fig. 4) which are normalised using the same method as the two sets of six 2MASS strips in Fig. 5.

### 3.3 $|b| \geq 30^\circ$ 2MASS galaxy counts

To investigate the local galaxy distribution further, we have extended the area studied from the two sets of six strips to an area over the galactic caps to  $|b| \geq 30^\circ$  (see Fig. 6). Moving to these larger areas, we see that the hole in the SGC persists with a deficiency of  $\sim 30$  per cent with respect to the homogeneous model at  $K_s = 11.13$ , similar to those seen in the SGC strips. In the NGC, the approximate homogeneous trend observed in the  $B \leq 17.5$  2dF NGP  $n(z)$  is replaced by counts which are underdense by  $\sim 18$  per cent at  $K_s = 11.13$ , indicating the possible presence of a large void in the NGC as well as the SGC. It is interesting to note

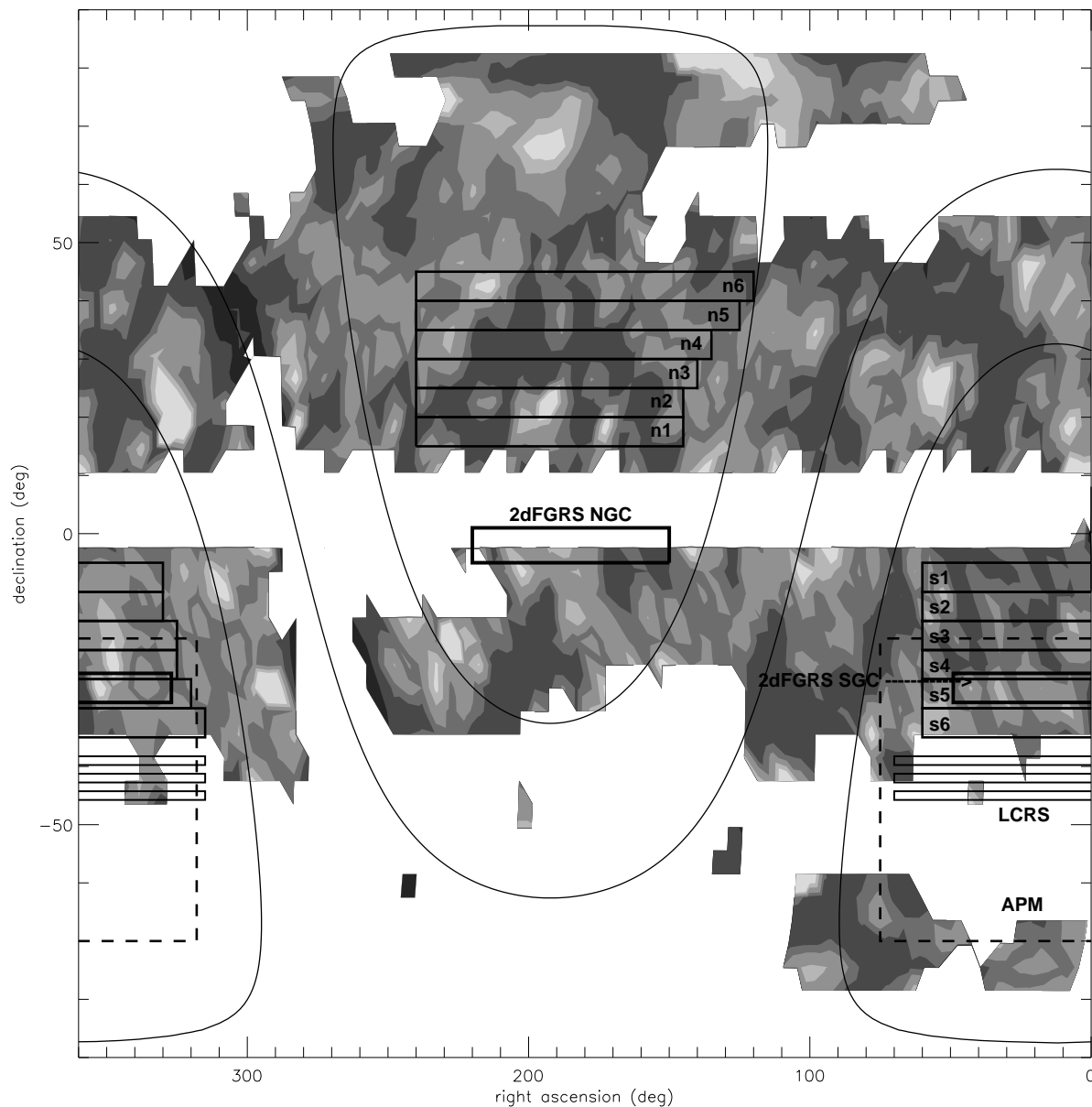


**Figure 7.** The ratio of 2MASS galaxies in the ranges  $11.38 < K_s < 12.38$  and  $12.88 < K_s < 13.38$  taken for  $25 \text{ deg}^2$  areas as a function of position on the sky. The least shaded regions indicate shallow counts corresponding to a galaxy distribution of  $< 50$  per cent with respect to the homogenous prediction, with progressively darker areas indicating density levels of  $< 60$  per cent,  $< 80$  per cent,  $< 100$  per cent,  $< 200$  per cent and  $> 200$  per cent; these contour levels are used to emphasise the underdense regions of interest. Also shown are the 2MASS strip and galaxy survey fields of interest. Galactic longitude lines are shown for  $b = -30^\circ$ ,  $0^\circ$  and  $30^\circ$ . For reference, the Coma galaxy cluster is at  $\alpha = 195^\circ$ ,  $\delta = +28^\circ$  and the Shapley cluster is at  $\alpha = 202^\circ$ ,  $\delta = -27^\circ$ .

also that the counts in both hemispheres display comparable deficiencies of  $\sim 20$  per cent at  $K_s = 11.63$ . Clearly as the northern area gets bigger, the picture gets more complicated with areas of underdensity also appearing as in the SGC.

Due to the complexity of the mask for the 2MASS second incremental release, we have found it difficult to estimate the actual solid angle surveyed and have simply normalized the counts in Fig. 6 to the mean number density observed in the corresponding set of strips in Fig. 5 at the

$K_s = 13.13$  half magnitude bin; this is likely to be a reasonable procedure since the implied solid angle of the 2MASS mask over the galactic caps is only a factor of  $\sim 2$  larger than the combined effective area of the strips.

Thus, the north–south asymmetry observed in the 2dFGRS  $n(z)$  and optical magnitude counts and the 2MASS counts selected for 2dF declination strips appears to be in disagreement with the 2MASS counts over the galactic caps.

A possible explanation comes from a more detailed analysis over larger areas provided in the next section.

### 3.4 Mapping the Local Galaxy Distribution

Finally, we wish to investigate the form and extent of the local hole at a higher resolution and over a larger area than the  $|b| \geq 30^\circ$  areas while avoiding calculations of the effective area. It is clear from the 2MASS counts and the variable  $\phi^*$  models that an essential signature for a local hole at  $\sim 150 h^{-1}$  Mpc distance is the steep slope between  $K_s \sim 11$  and  $\sim 13$ . We have therefore examined the 2MASS galaxy counts over the entire available area in this magnitude range binned in  $25 \text{ deg}^2$  areas with a constant declination range of  $5^\circ$ . With the distances being explored at these magnitude limits, this amounts to a smoothing on a linear scale of  $\sim 10 h^{-1}$  Mpc. For each area we then calculated the ratio of the number of galaxies in the whole magnitude bin  $11.38 < K_s < 12.38$ , to that in the half-magnitude bin  $12.88 < K_s < 13.38$ , a procedure in which the two numbers are similar and the error on the ratio reasonable. Finally, we divided this ratio by the predicted ratio of the homogeneous model. This ‘slope statistic’ is then a measure of how steep or shallow the counts are relative to the homogeneous slope. Equivalently, if we assume the counts in  $25 \text{ deg}^2$  areas are approximately homogeneous by  $K_s = 13.13$ , the ratio is then just the observed count in the  $K_s \sim 11.88$  half magnitude bin as a fraction of that predicted by the homogeneous model; it then indicates the extent to which the area is underdense or overdense at distances of  $\lesssim 150 h^{-1}$  Mpc. Clearly, for this latter interpretation of the ‘slope statistic’ there is some error, as the smoothing area is an order of magnitude smaller than the declination strips of the previous section and so a uniform number density in the  $K_s = 13.13$  bin, as is observed in the strips, cannot be assumed. However, it may at least prove useful as a qualitative probe of local density inhomogeneities. Fig. 7 is a contour map of this statistic.

A particular advantage of this technique is that it is independent of an accurate determination of the effective area, while allowing us to probe the galaxy distribution over large contiguous areas of sky in the volume below  $\sim 150 h^{-1}$  Mpc. However, galaxy magnitudes at low galactic latitudes of  $|b| < 30^\circ$  begin to be effected by significant extinction even in the  $K$ -band, and the mapped statistic in these regions is unreliable for the purposes here.

The use of the map in Fig. 7 as an indicator of inhomogeneities in the distribution of galaxies on the sky is supported by, first, its ability to pick out known clusters at distances of  $\lesssim 150 h^{-1}$  Mpc; the Coma cluster and its associated supercluster can clearly be seen; the Shapley cluster also appears as a high density area. Secondly, we also see generally good agreement with the results in the previous section for the declination strips. This is typified by the more patchy form of the galaxy distribution in the NGC than in the SGC, where overdense regions exist around the pole but accidentally cancel with surrounding underdensities to produce low counts in four of the NGC strips.

From Fig. 7 it can also be observed that the very large ‘local hole’ that we have been exploring in the SGC is a coherent aggregation of smaller holes. In particular, we see that the 2dF SGC area lies in a general region of such holes

or voids, with a remarkably large area of right ascension between  $280^\circ$  and  $50^\circ$  and declination between  $-2^\circ$  and  $-35^\circ$ .

Fig. 7 also supports the relative similarity of the NGC and SGC cap counts for  $|b| > 30^\circ$  with large regions of shallow counts in the NGC countered only by the area of steeper counts at the NGP. It is also now apparent why the counts in the northern strip 3 have a much flatter slope than the southern strips and the northern and southern cap counts, since there appears to be a particularly dense region in the galaxy distribution over the NGP, surrounded by a region of much shallower counts, further supporting the possibility of a large void in the NGC.

Fig. 7 also indicates that the galaxy distribution is highly varied as might be expected with the cosmic web smoothed on scales of  $\sim 10 h^{-1}$  Mpc. In particular, individual deep holes, underdense by as much as  $\gtrsim 50$  per cent, with sizes of  $\sim 10\text{--}20^\circ$  can also be observed. Considering the depth of the survey this corresponds to a linear scale of  $\sim 20\text{--}60 h^{-1}$  Mpc, similar to the scale of voids found using large redshift surveys (e.g. Bellanger & De Lapparent, 1995).

## 4 SUMMARY AND CONCLUSIONS

In this paper, we first reviewed the evidence from APM and 2dFGRS optical number-magnitude counts that the  $B < 18$  mag. counts particularly in the SGC are steeper than expected on the basis of simple homogeneous models. One possible interpretation is that this is caused by a large local hole in the distribution of galaxies. However, other possible interpretations are that the effect is caused by evolution or poor photographic photometry. New data, principally the 2dFGRS  $n(z)$  and the 2MASS second incremental release, have therefore been used to discriminate between these various possibilities. With the 2dFGRS, any local hole can be sought in the redshift distribution directly and the 2MASS  $K_s$  counts can be used as a check of the steepness of local galaxy counts in a band where a linear detector has been used and the effects of evolution are likely to be less than in the  $B$ -band.

The 2MASS data is not in its final form and there are problems in particular with an uncertain mask in various areas of the survey. We therefore first made a detailed analysis of the 2MASS data in the NGC and SGC 2dFGRS fields each of  $\sim 300 \text{ deg}^2$  area to check for the hole in the south and investigate the previous apparent north–south asymmetry in the counts.

Then we extended this approach to a wider area of the NGC and SGC, first using strip counts in  $\sim 1800 \text{ deg}^2$  areas near each of the galactic poles in each hemisphere, then overall NGC and SGC counts based on all available 2MASS areas with  $|b| \geq 30^\circ$ . Finally, using a 2MASS count ‘slope statistic’, we made a higher resolution ( $\sim 10 h^{-1}$  Mpc) map to investigate the detailed form of the large-scale structure to an average depth of  $\sim 150 h^{-1}$  Mpc, again over the full available 2MASS area.

The results are summarised as follows:-

- The 2MASS  $K_s$  number count in the 2dFGRS SGC field is significantly steeper than in the 2dFGRS NGC field, consistent with previous results in the  $B$ -band.



- Large holes are seen in the galaxy distribution in the 2dFGRS SGC  $B \leq 17.5$   $n(z)$  out to  $z < 0.1$  which are not seen in the NGC 2dFGRS  $B \leq 17.5$   $n(z)$ .

- Variable  $\phi^*$  number count models which track the 2dFGRS  $n(z)$ 's give a good fit to the  $K_s$ -band galaxy counts in both the NGC and SGC 2dFGRS areas, suggesting that the steep SGC counts are due to the holes in the 2dFGRS SGC  $n(z)$ .

- The six 2MASS SGC strip counts over an  $\sim 2000$  deg<sup>2</sup> area consistently show the same underdensity as seen in the 2dFGRS SGC field. Counts over a similar area in the NGC show a more varied behaviour with some strips being higher than even the homogeneous model and others starting to show the same level of underdensity as seen in the SGP.

- 2MASS  $K_s$  counts over the whole SGC and NGC areas with  $|b| \geq 30^\circ$  indicate an underdensity in the SGC which is only slightly less than in the 2dFGRS SGC field and an increased underdensity in the NGC area.

- Examining the 2MASS counts at a higher resolution with the 'slope statistic' reveals a more patchy form to the galaxy distribution in the NGC than in the SGC. In particular, overdensities associated with the Coma and Shapley clusters can clearly be detected. These areas are surrounded by regions of underdensity resulting in the reasonably homogeneous counts seen in the 2dFGRS NGC field and the six NGC strips. The SGC shows more evidence of contiguous underdensity again consistent with the steep  $K_s$  counts seen in the 2dFGRS SGC field and the six SGC strip counts.

- Using the evidence from 2MASS using the 'slope statistic' and the six SGC strips, and also the underdensity seen in the LCRS (Shectman et al. 1996), we conclude that an underdensity of  $\sim 30$  per cent in the SGC extends over at least  $280^\circ < \alpha < 50^\circ$  and  $-45^\circ < \delta < 0^\circ$  to  $\gtrsim 150 h^{-1}$  Mpc. This corresponds to a linear size across the sky of  $\sim 200 h^{-1}$  Mpc.

- The 'slope statistic' map also supports the form of the  $b > 30^\circ$  counts, indicating large regions of underdensity in the NGC away from the NGP and moderated only by the effect of the Coma cluster at the pole, indicating the possible presence of a huge, connected local underdensity present in both galactic caps of scale  $\gtrsim 300 h^{-1}$  Mpc.

## ACKNOWLEDGMENTS

This publication makes use of data products from the Two Micron All Sky Survey, which is a joint project of the University of Massachusetts and the Infrared Processing and Analysis Centre/California Institute of Technology, funded by the Aeronautics and Space Administration and the National Science Foundation. We thank Tom Jarrett for his helpful information on the 2MASS mask. We would also like to thank Carlton Baugh and Shaun Cole for useful discussions, and Richard Bower and Phil Outram for technical help.

## REFERENCES

Baugh, C.M., Branchini, E., Cole, S., Jenkins, A.R., & Frenk, C.S. 2002, in prep.  
 Bellanger, C. & De Lapparent, V. 1995, ApJ, 455, L103  
 Bruzual, A.G. & Charlot, S. 1993, ApJ, 405, 538  
 Buswell, G.S. et al. 2002, in prep.

Cole, S. et al. 2001, MNRAS, 326, 255  
 Colless, S. et al. 2001, MNRAS, 328, 1039  
 De Lapparent, V., Geller, M.J. & Huchra, J.P. 1988, ApJ, 332, 44  
 Folkes, S. et al. 1999, MNRAS, 308, 459  
 Frith, W.J. 2001, M.Sci. Thesis, Univ. of Durham  
 Gardner, J.P., Sharples, R.M., Carasco, B.E. & Frenk, C.S. 1996, MNRAS, 282, L1  
 Glazebrook, K., Peacock, J.A., Miller, J.A. & Collins, C.A. 1995, MNRAS, 275, 169  
 Huang, J.S., Cowie, L., Gradner, J.P., Hu, E.M., Songalia, A., & Wainscoat, R.J. 1996, ApJ, 476, 12  
 Jarrett, T.H., Chester, T., Cutri, R., Schneider, S., Skrutskie, M., & Huchra, J.P. 2000, AJ, 119, 2498  
 Loveday, J., Peterson B.A., Maddox, S.J. & Efstathiou, G. 1996, ApJS, 107, 201  
 Loveday, J. 2000, MNRAS, 312, 517  
 Maddox, S.J., Sutherland, W.J., Efstathiou, G. & Loveday, J., 1990, MNRAS, 243, 692  
 Maddox, S.J., Efstathiou, G. & Sutherland, W.J., 1990, MNRAS, 246, 433  
 Metcalfe, N., Fong, R. & Shanks, T. 1995, MNRAS, 274, 769  
 Metcalfe, N., Shanks, T., Campos, A., McCracken, H.J. & Fong, R. 2001, MNRAS, 323, 795  
 Norberg, P. et al. 2001, astro-ph/0111011  
 Pimblet, K.A., Smail, I., Edge, A.C., Couch, W.J., O'Hely, E. & Zabludoff, A.I. 2001, MNRAS, 327, 588  
 Ratcliffe, A., Shanks, T., Broadbent, A., Parker, Q.A., Watson, F.G., Oates, A.P., Fong, R. & Collins, C.A. 1996, MNRAS, 281, L47  
 Shanks, T. 1990, in The Galactic and Extragalactic Background Radiations, S. Bowyer & C. Leinert, Dordrecht:Kluwer, 269  
 Shectman, S.A., Landy, S.D., Oemler, A., Tucker, D.L., Lin, H., Kirshner, R.P., & Schechter, P.L., 1996, ApJ, 470, 172  
 Zucca, E. et al. 1998, astro-ph/9805195